Open Access **Baghdad Science Journal** **P-ISSN: 2078-8665**
Published Online First: September 2022 **2023, 20(2): 616-621** **E-ISSN: 2411-7986**

DOI: http://dx.doi.org/10.21123/bsj.2022.6730

Photonic Crystal Fiber Pollution Sensor Based on the Surface Plasmon Resonance Technology

Fatima Fadhil Abbas* ***Soudad S. Ahmed***

Department of Physics, College of Science, University of Baghdad, Baghdad, Iraq.
*Corresponding author: fatimafadhel.Abaas1104@sc.uobaghdad.edu.iq
E-mail addresses: soudadbassam@gmail.com

Received 5/11/2021, Revised 2/4/2022, Accepted 4/4/2022, Published Online First 20/9/2022
Published 1/4/2023

Abstract

Photonic Crystal Fiber (PCF) based on the Surface Plasmon Resonance (SPR) effect has been proposed to detect polluted water samples. The sensing characteristics are illustrated using the finite element method. The right hole of the right side of PCF core has been coated with chemically stable gold material to achieve the practical sensing approach. The performance parameter of the proposed sensor is investigated in terms of wavelength sensitivity, amplitude sensitivity, sensor resolution, and linearity of the resonant wavelength with the variation of refractive index of analyte. In the sensing range of 1.33 to 1.3624, maximum sensitivities of 1360.2 nm/RIU and 184 RIU^{-1} are achieved with the high sensor resolutions of 7 $\times 10^{-5}$ RIU and 5.4× 10^{-5} RIU using wavelength and amplitude interrogation methods, respectively. The proposed sensor could be established to detect various refractive index (RI) of pollutions in water.

Keywords: Optical Fiber Sensor, Optical Fiber Surface Plasmon Resonance, Photonic Crystal Fiber, Polluted Water**.**

Introduction:

PCFs are divided into two categories depending on their light-guiding mechanisms: solid core photonic crystal fibers (SC-PCFs), which use a Modified Total Internal Reflection (MTIR) and hollow core photonic crystal fibers (HC-PCFs) which use the Photonic Band Gap (PBG) effect[1].

PCF have received a lot of interest in recent years due to unique features that are not attained in traditional optical fibers such as small size, which reduces electromagnetic interferences as well as high sensitivity, electrical passiveness, improved stability and fast optical response [2]. Furthermore, PCF configuration is very flexible, with several parameters to control: including the shape and diameter of the air hole, the lattice pitch, and the refractive index of the glass[3,4]. In contrast, other physical characteristics may also be measured, including temperature, pressure, acceleration and monitoring of hydrocarbons, etc.[5].

SPR refers to surface Plasmon resonance and is defined as an optical phenomenon that occurs when p - polarized light excites a charge density oscillation at the metal-dielectric interface by achieving the phase matching state between the p - polarized light and SP[6].Combining the advantages of PCF technology with plasmonic science, PCF-SPR sensors have been developed, for a wide range of potential applications such as water testing[7], food safety, solution concentration measurement[8], environmental monitoring, biomedical treatment[9], gas detection, medical diagnostics, and so on[10]. The sensing mechanism of PCF-SPR is generated by means of an evanescent field. When light of a specific wavelength is incident on the fiber core of the PCF and some of the fields pass through the cladding, an evanescent field is formed. When evanescent fields interact with free electrons in a plasmonic metal layer like silver, gold, copper, or aluminum, the surface plasmon wave is created. The core guided and Surface Plasmon Polariton SPP_modes are now coupled, and the core guidance mode's RI (real value) is similar to that of the SPP mode, which is known as phase matching [11,12]. PCF-SPR technology overcomes conventional prism-based SPR sensing challenges including bulky construction, accurate incident angle as well as a large number of moving mechanical components, which limit the remote sensing and broad range of

applications [13]. Based on sensor evaluation, there are two different types of sensing approaches: internal sensing approaches and external sensing approaches. The analyte is used to fill the air hole in the internal sensing or nanowire-based sensing, and a metal layer is coated around the core. Placing the plasmonic material externally is another approach to external sensing medium, such as microchannel sensors, slit sensors, and D-shape [14].

Rifat et al., 2018 investigated an internally silver-coated PCF as an SPR sensor with a wavelength sensitivity (S_W) equal to 300 nm/RIU and an amplitude sensitivity (S_A) equal to 418 RIU^{-1} within a sensing range of 1.46–1.49 RIU[15]. The same researchers improved the sensitivity and detection range of the internally coated sensor by introducing a bigger cavity inside the fiber core[12]. Mahmood et al., 2018. proposed PCF-SPR sensor with maximum sensitivity of 164.3 nm/RIU in the sensing range of analyte RI 1.33–1.3431, which uses plasmonic material such as gold to coat air holes and filled with analyte sample [16]. Muhammed et al. presented a hollow core photonic crystal fiber as a water quality sensor with a core of PCF filled with various concentrations of H_2O_2 and D_2O in water, with relative sensitivity decreasing with increasing concentration and varying between 97 percent and 67 percent for H_2O_2 solution and between 80 percent and 41 percent for D_2O, where relative sensitivity is dependent on effective refractive index profile[7].

In this study, however, sensor performance was significantly improved by using an internal sensing approach. As a result, obtaining effective coupling between the core - guiding mode and the SPP mode can improve the sensor's performance. Up to date, most demonstrated PCF- SPR sensors have also been mathematically investigated, and the majority of reported PCF conformations were difficult to fabricate because to their small diameter of air hole, complicated structure, and small diameter of fiber. In this study, the numerical resulted are studied by using the finite element method (FEM) through COMSOL MULTIPHYSICS (v 5.4) to investigate performance parameter of ESM-12-02 PCF based on SPR. The cross section of fabricated PCF consists of a solid core surrounded by a periodic of six arrays of air holes. The hole on the right side of solid core is selected and coated with a chemically stable material such as gold before being filled with analyte to prevent the oxidation due to the infiltration of air holes with polluted water samples.

Theoretical Analysis and Sensor Design

Sellmeier Equation

In the construction of the proposed sensor, essentially silica is used. All of the holes in the structure are empty, i.e., filled with air. The refractive index of silica is determined by the eq.1 [17]:

$$N_{silica} = 1 + \frac{a_1\lambda^2}{\lambda^2 - b_1} + \frac{a_2\lambda^2}{\lambda^2 - b_2} + \frac{a_3\lambda^2}{\lambda^2 - b_3} \ldots\ldots\ldots\ldots 1$$

N is the refractive index of silica that depends on wavelength, λ is the wavelength in μm, and the Sellmeier coefficients for silica are (a_1, a_2, a_3) and (b_1, b_2, b_3)respectively .

a_1=0.6961663, a_2=0.4079426, a_3= 0.8974794, c_1=0.0684043 μm^2, c_2= 0.1162414 μm^2 and c_3=9.896161 μm^2.

Drude–Lorentz Model

Drude model is not suited at higher frequency regime for calculating the real and imaginary part of dielectric constant (ε). The interband effect (IB) may be nullified as a sum of Lorentzian functions, the dielectric function depending on a frequency can simply be expressed as $\varepsilon(\omega)=\varepsilon Drude(\omega)+\varepsilon IB(\omega)$ [18]. Thus, the dispersion relation of Au as the noble metal could be expressed using Drude-Lorentz model as Eq.2

$$\varepsilon_{Au} = \varepsilon_\infty - \frac{\omega_D^2}{\omega(\omega + j\gamma_D)} - \frac{\Delta\varepsilon.\Omega_L^2}{(\omega^2 - \Omega_L^2) + j\Gamma_L\omega} \ldots\ldots\ldots\ldots 2$$

Where ε_{Au} denotes the permittivity of the gold material and ε_∞ is the gold permittivity at a high frequency that has a value of 5.9673. ω is the angular frequency which may be expressed as $\omega = 2\pi c/\lambda$, c is the velocity of light in vacuum. $\omega_D/2\pi$ =2113.6 THz and $\gamma_D/2\pi$=15.92 the plasma and damping frequency respectively .Δε is the weighting factor and equal to1.09. $\Gamma_L/2\pi$ = 104.86 THz is the spectral width and $\Omega_L/2\pi$=650.07 THz is the oscillator strength of the Lorentz oscillators.

Structural Design and Analysis

Photonic crystal fiber (PCF) model (ESM-12) made by NKT Photonics has always been an endless single mode fiber with outer diameter of 125μm and is compatible with all common fiber tools.Fig.1. a shows a scanning electron microscope (SEM) image of a fabricated (ESM-12) PCF with a lattice constant (Λ) of 7.8 μm and an air hole diameter (d) of 4.5 μm. Fig.1.b illustrations a schematic of the proposed PCF-SPR sensor, which was created using the Finite Element method (FEM). Perfectly Matched Layer (PML) is circular layer with thickness 12μm in the proposed structure was used as the boundary condition for absorbing scattering lights toward the surface of fiber. Convergence tests also were successfully completed, optimized with the PML thickness and mesh size for more accurate results. The analyte is filled into the air-hole (d_1), which is then coated with 40 nm thickness layer of plasmonic material such as gold.

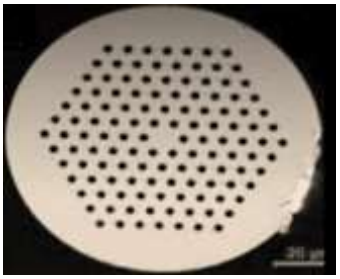

Figure 1.a. (SEM) image of the (ESM -12)PCF

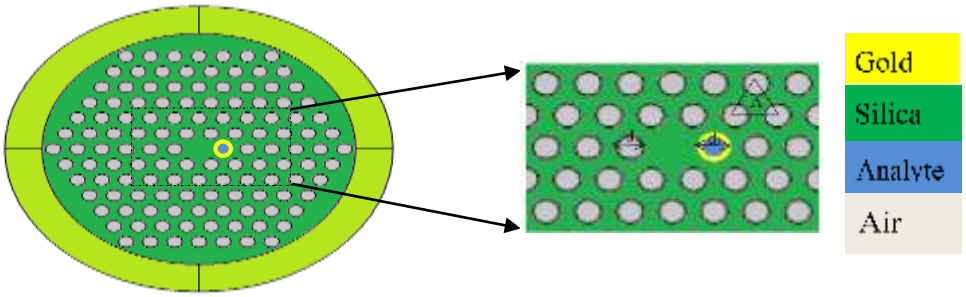

Figure1. b. cross section views of (ESM- 12) PCF

Electrical -filed distribution of fundamental core - guiding mode, (phase matching) core mode and 2nd SPP mode for y-polarization mode are shown in Figs. 2(a)–2(c), respectively. The phase matching between core guiding mode and surface Plasmon polarization (SPP) mode produces resonance at a specified wavelength for a given analyte/sample. Fig.2.d shows the dispersion relation between the second SPP mode and the fundamental core mode when RI is 1.36, t_{Au} = 40 nm around the resonant frequency in y-polarizations mode. The confinement loss of the propagation mode of the overall structure is also shown in fig.2(d) (black line). At the resonant wavelength of 626 nm, where the core guided fundamental mode and the 2nd SPP mode intersect, a sharp loss peak occurs. As a result, the basic core mode transfers the most energy to the SPP mode. The confinement loss can be obtained by using Eq.3[19]:

$$\alpha\left(\frac{\mathrm{dB}}{\mathrm{cm}}\right) = 8.686 \times k_0 \,\mathrm{Im}(n_{eff}) \times 10^4 \ldots\ldots 3$$

where Im(n_{eff}) is the imaginary part of the effective mode index and k_0 is the wave number.

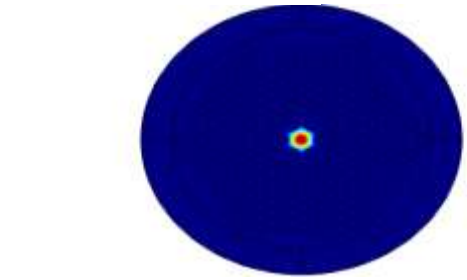

(a)

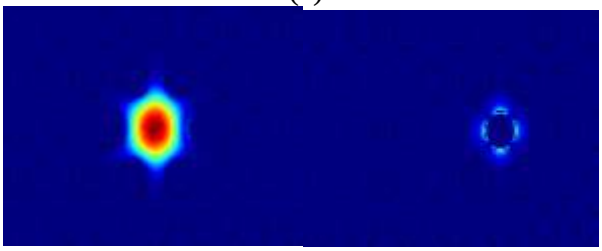

(b) (c)

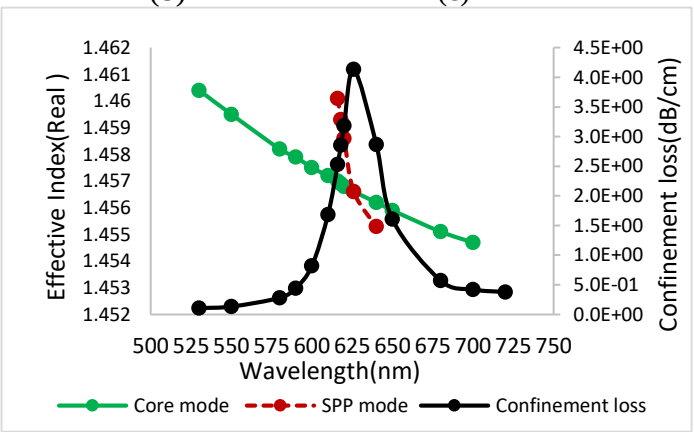

(d)

Figure 2. Electric field distributions at n_a =1.3624 in (a) core-guided mode, (b) phase-matching condition, (c) 2ndSPP mode (y-polarized), and (d)dispersion relation between

core guiding mode and the second Surface plasmon mode.

These results were obtained using a phase matching condition and a refraction index of 1.3624 for the analyte. The loss depth is greatly influenced by small changes in the analyte RI. The proposed PCF sensor's loss spectrum with different n_a is displayed in Fig.3. As the loss depth increases, the peak shifts toward longer wavelengths (redshift). This is because an increased effective refractive index(n_{eff}) of surface plasmon mode modulate phase matching point with reduces the difference between core guided mode and plasmon mode which makes the coupling efficiency stronger. For n_a =1.3624 at 626 nm, the maximum loss depth occurs and equal to 4.13(dB/ cm) and the power exchange between the core and SPP modes increases as the loss depth increases, owing to an increase in RI of analyte resulting in a narrow resonant spectrum.

When the refractive index of the analyte is 1.33,1.3433,1.3542 and 1.3624 the resonant peaks of wavelength is 580,600,610 and 620nm respectively, which are shown in Fig.4 with linear fitting.

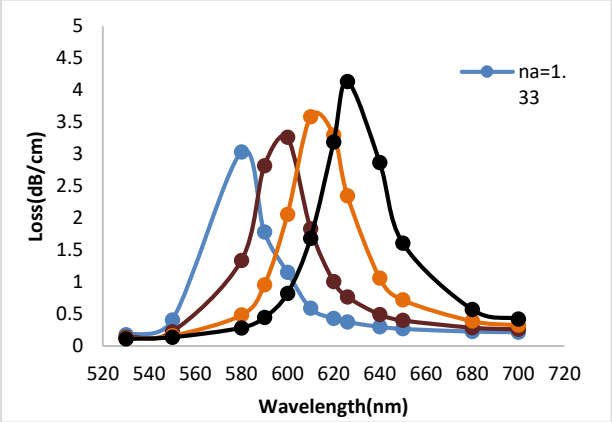

Figure 3. The confinement loss spectrum of the proposed PCF SPR sensor variation with increase analyte RI from 1.33 to 1.3624.

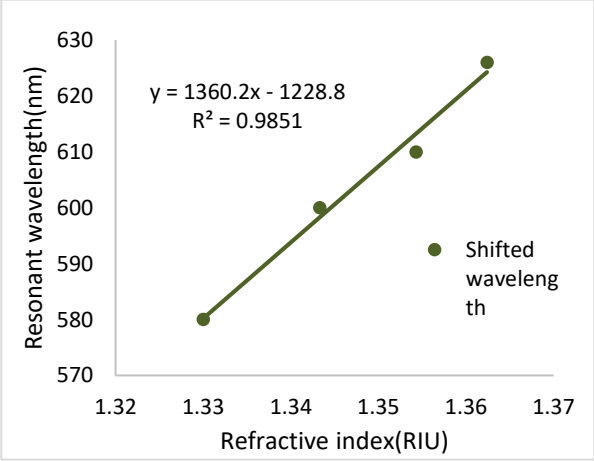

Figure 4. Resonant wavelength versus refractive index

The suggested sensor's performance can be evaluated using both interrogation methods: wavelength and amplitude interrogation methods. The wavelength sensitivity may be calculated using the Eq.4[19]:

$$S_W(\lambda) = \frac{\Delta\lambda_{peak}}{\Delta n_a} \quad \ldots\ldots\ldots\ldots\ldots\ldots 4$$

$\Delta\lambda_{peak}$ and Δn_a denote the shift in resonance peaks and analyte RI, respectively.

For n_a of 1.33,1.3433, and 1.3542, the proposed sensor has wavelength sensitivity of 1360.2 nm/RIU^{-1}. The peaks of resonant wavelength are 20, 10, and 16 nm, respectively, for analyte RI variations of 1.33–1.3433, 1.3433–1.3542, and 1.3542-1.3624. Another important parameter is the sensor's resolution, which describes how the sensor detects a small change in the analyte RI. Resolution (R) of proposed senser was given by Eq.5 [20]:

$R = \Delta n_a \times \Delta\lambda_{min} / \Delta\lambda_{peak}$ [RIU] …….5

Where n_a represents analyte RI variation, the minimum spectral resolution is represented by $\Delta\lambda_{min}$ and $\Delta\lambda_{peak}$ represents peak shift of the maximum resonant wavelength. The maximum resolution of proposed sensor is 5.125×10^{-5} RIU, assuming Δn_a = 0.0082, $\Delta\lambda_{min}$= 0.1, $\Delta\lambda_{peak}$= 16 nm, and n_a =1.3642. The following Eq.6 can be used to calculate the sensor's amplitude sensitivity [15]:

$$S_A(\lambda) = -\frac{1}{\alpha(\lambda,n_a)}\frac{\partial\alpha(\lambda,n_a)}{\partial n_a} \quad [\text{RIU}^{-1}] \ldots\ldots\ldots\ldots 6$$

Where α (λ, n_a) represent the confinement loss of analyte at a given refractive index RI and ∂α (λ, n_a) denotes the difference in confinement loss between two analytes with adjacent refractive indexes. Fig 5. shows the amplitude sensitivity of various analyte refractive index RI. The maximum amplitude sensitivity was 95.6 RIU^{-1}, 179 RIU^{-1}, and 184 RIU^{-1}, respectively, when the analyte RI variation range was 1.33-1.3433, 1.3433-1.3542, and 1.3542-1.3624.

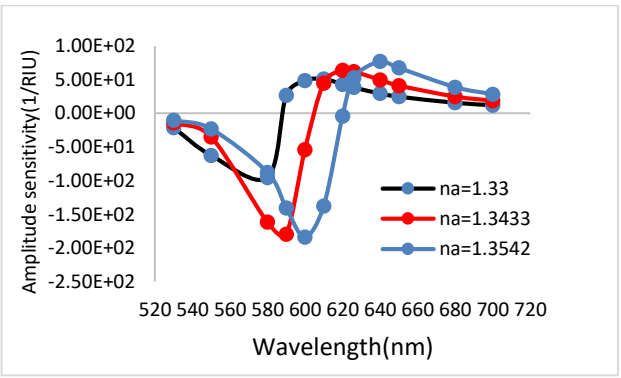

Figure 5. Amplitude sensitivity as a function of wavelength when refractive index n_a of analyte increasing from 1.33 to 1.3624

Conclusion:

Photonic Crystal Fiber sensor based on surface Plasmon Resonance (PCF-SPR) numerically is exploited in this work to detect polluted water sample by coating air hole in the right side of PCF core with gold layer. The unknown analyte can be detected from the resonant wavelength or the peak of confinement loss spectrum matching the real part of effective index of core guiding mode and surface plasmon mode. The sensor parameters of the fundamental mode have been studied by employing the FEM. The maximum wavelength sensitivity is 1360.2 nm/RIU and amplitude sensitivity is 184 RIU^{-1} in the sensing range of 1.33 (distilled water)-1.3624 (polluted water) is found. The suggested sensor may be used as a pollution sensor due to its simple structure and great sensing characteristics.

Authors' declaration:

- Conflicts of Interest: None.
- We hereby confirm that all the Figures and Tables in the manuscript are mine ours. Besides, the Figures and images, which are not mine ours, have been given the permission for re-publication attached with the manuscript.
- Ethical Clearance: The project was approved by the local ethical committee in University of Baghdad.

Authors' contributions statement:

S. S. A., was responsible for design the experiment, revision and proofreading of the manuscript. F. F. A., was designed algorithm of experiment, writing the manuscript and analysis the results.

Reference:

1. Taher H J. Low loss in Gas filled Hollow core photonic crystal fiber. Baghdad Sci J.2010;7(1):129-138.
2. Ademgil H, Haxha S. PCF Based Sensor with High Sensitivity. High Birefringence and Low Confinement Losses for Liquid Analyte Sensing Applications. Sensors. 2015; 15:31833-31842.
3. Maidi AM, Yakasai I, Abas PE, Nauman MM, Apong R A , Kaijage S, et al . Design and Simulation of Photonic Crystal Fiber for Liquid Sensing. Photonics 2021; 8(1), 16.
4. Buczynski R. Photonic crystal fibers. Acta Phys Pol. A .2004; 106, 141–167.
5. Alok Kumar Paul. Design and analysis of photonic crystal fiber plasmonic refractive Index sensor for condition monitoring of transformer oil. OSA Continuum. 2020; 3: 2253-2263.
6. Sultan M F, Al-Zuky A A, Kadhim S A. Surface Plasmon Resonance Based Fiber Optic Sensor: Theoretical Simulation and Experimental Realization. ANJS. 2018; Mar ,21(1):65-70.
7. Muhammed N F, Mahmood A I, Kadhim Sh A, Naseef I A. Simulation Design of Hollow Core Photonic Crystal fiber for Sensing Water Quality.2020; May, J Phys: Conf Ser. 1530 012134.
8. Maheswaran S, Kuppusamy P, Ramesh S, Sundararajan T, Yupapin P, Refractive index sensor using dual core photonic crystal fiber–glucose detection applications. Results Phys. 2018; 11: 577–578.
9. Gatea M AF, Jawad A H . Thermoplasmonic of single Au@SiO2and SiO2@Au core shell nanoparticles in deionized water and poly-vinylpyrrolidone matrix. Baghdad Sci J.2019;Jun,16(2): 0376.
10. Yuan H, Ji W, Chu S, Liu Q, Qian S, Guang J, et al. Mercaptopyridine functionalized gold nanoparticles for fiber-optic surface plasmon resonance Hg2+ sensing. ACS Sens. 2019; 4(3), 704–710.
11. Rahman MT, Datto S, Sakib M N. Highly sensitive circular slotted gold-coated micro channel photonic crystal fiber based plasmonic biosensor. OSA Continuum. 2021;4: 1808-1826.
12. Rifat A A, Haider F, Ahmed R, Mahdiraji G A, Adikan F R M, Miroshnichenke E. Highly sensitive selectively coated photonic crystal fiber-based plasmonic sensor. Opt.Lett.2018; 43(1):891-894.
13. Rifat A A, Photonic crystal fiber based plasmonic sensors. Sens. Actuators. B. 2017; 243: 311–325.
14. Rifat A A, Hasan Md R, Ahmed R, Butt H. Photonic crystal fiber-based plasmonic biosensor with external sensing approach. J Nanophoton. 2017;12(1): 012503.
15. Rifat A A, Mahdiraji G A, Chow D M, Shee Y G, Ahmed R, Adikan F R M .Photonic crystal fiber-based surface plasmon resonance sensor with selective analyte channels and graphene-silver deposited core. Sensors.2015; 15: 11499–11510.
16. Mahmood I A, Ibrahim R Kh, Aml I Mahmood, Ibrahim Z Kh. Design and simulation of surface plasmon resonance sensors for environmental monitoring. J Phys.: Conf Ser. 2018; 1003: 012118.
17. SellMeier W, Zur erklärung der abnormen farbenfolge im spectrum einiger substanzen. Ann Phys Chem. 1871; 219(6): 272–282.
18. Vial A, Grimault A S, Macías D, Barchiesi D, De La Chapelle M L. Improved analytical fit of gold dispersion: application to the modeling of extinction spectra with a finite-difference time-domain method. Phys Rev B. 2005;71(8): 085416.
19. Wang G., Li S, An G, Wang X, Zhao Y, Zhang W, Chen H. Highly sensitive D shaped photonic crystal fiber biological sensors based on surface Plasmon resonance. Opt Quantum Electron. 2016: 48 1–9.

20. Rifat A A, Mahdiraji G A, Sua Y M, Ahmed R, Shee Y G, Adikan F R M. Highly sensitive multi-core flat fiber surface plasmon resonance refractive index sensor. Opt. Express.2016; 24: 2485-2495.

متحسس التلوث باستخدام الالياف الضوئية البلورية استنادا الى تقنية رنين بلازمون السطح

فاطمه فاضل عباس **سؤدد سلمان احمد**

قسم الفيزياء، كلية العلوم ، جامعه بغداد، بغداد ، العراق.

الخلاصة:

تم اقتراح الألياف البلورية الضوئية (PCF) بناءً على تأثير رنين البلازمون السطحي (SPR) للكشف عن عينات المياه الملوثة. يتم توضيف خصائص الاستشعار باستخدام طريقة العناصر المحدودة. الفجوة على الجانب الأيمن من قلب PCF مطلية بمادة الذهب المستقرة كيميائيًا لتحقيق عملية الاستشعار. تم فحص معلمات أداء المستشعر المقترح من حيث حساسية الطول الموجي ، وحساسية السعة ، ودقة المستشعر ، والعلاقة الخطية لطول موجة الرنين مع تغيرفي معامل الانكسار العينات . في نطاق الاستشعار من 1.33 إلى 1.3624 ، تم تحقيق اقصى حساسية بلغت 1360.2 nm/RIU و $184\ RIU^{-1}$مع دقة مستشعر عالية بلغت 7×10^{-5} RIU و 5.4×10^{-5} باستخدام طرق التحقيق كالطول الموجي والسعة على التوالي. يمكن تصنيع المستشعر المقترح لإكتشاف الملوثات في المياه عن طريق ايجاد معاملات انكسارها .

الكلمات المفتاحية: متحسس الالياف البصرية، رنين بلازمون السطح الليف البصري،ا لالياف البلورية الضوئية، المياه الملوثة